

# Sensitivity analysis of limit cycles of Navier–Stokes equations by the Harmonic–Balance method

Javier Sierra\*

UNISA – University of Salerno, Fisciano Italy  
UPS-IMFT – Paul Sabatier University – Institute of Fluid Mechanics,  
Toulouse France

Pierre Jolivet

CNRS-IRIT, 2 rue Charles Camichel, 31071 Toulouse Cedex 7, France

Vincenzo Citro, Flavio Giannetti

UNISA – University of Salerno, Fisciano Italy

Sensitivity of periodic solutions of time-dependent partial differential equations are commonly computed using time-consuming direct and adjoint time integrations. Particular attention must be provided on the periodicity condition in order to obtain accurate results. Furthermore, stabilization techniques are required if the orbit is unstable. In this talk we will discuss an alternative methodology to evaluate the sensitivity of periodic flows via the Fourier–Galerkin method. Unstable periodic orbits are directly computed and continued without any stabilizing technique. Stability of the periodic state is determined via the Hill’s method: the frequency-domain counterpart of Floquet analysis. Sensitivity maps, used for open-loop control and physical instability identification, are directly evaluated using the adjoint of the projected operator. Furthermore, we propose an efficient and robust iterative algorithm for the resolution of underlying linear systems. The problem is solved with the FreeFEM library, in particular block matrices are interfaced with PETSc/SLEPc. Efficient preconditioning techniques are implemented to solve the underlying linear systems of the Newton iteration and they are put into test in the transition to a three-dimensional state in the periodic vortex-shedding past a circular cylinder. In addition, such a flow case allows the validation of the sensitivity approach by a systematic comparison with previous results presented in literature.

**Keywords:** Sensitivity, Fourier–Galerkin method, Floquet stability analysis, unstable periodic orbits

## I. METHODOLOGY

The generic autonomous class of evolution equations of the form:

$$\mathbf{B} \frac{\partial \mathbf{q}}{\partial t} = \mathbf{F}(\mathbf{q}, \nu), \quad \mathbf{q}(t + T) = \mathbf{q}(t), \quad (1)$$

where  $\mathbf{B}$  is a linear operator,  $\mathbf{F}$  is a nonlinear operator on a Hilbert space  $X$  with inner product  $\langle \cdot, \cdot \rangle$ , and  $\nu \in \mathbb{R}^p$  the set of parameters. In this way, both differential algebraic problems (DAE) and evolutionary partial differential equations (PDE) are included. whereas in finite dimensions we will generally consider  $\mathbb{R}^n$ . In the following, we assume that the nonlinear operator  $\mathbf{F}$  is of quadratic type, i.e.,  $\mathbf{F}(\mathbf{q}) = \mathbf{L}\mathbf{q} + \mathbf{N}(\mathbf{q}, \mathbf{q})$ , where  $\mathbf{L}$  and  $\mathbf{N}(\cdot, \cdot)$  are linear and quadratic nonlinear operators, respectively.

### A. The Fourier–Galerkin method for periodic boundary problems

The solution of eq. (1) is  $T$ -periodic. Therefore, it seems a natural choice to parametrize any  $T$ -periodic or-

bit  $\mathbf{q}^*$ , in a  $t \bmod T$  basis, i.e., a Fourier basis. For that purpose, let us consider the Fourier–Galerkin method, also denoted harmonic balance (HB) in literature [1, 2]. Fourier–Galerkin can be seen as a weighted residual approach for a periodic ansatz and weight functions. Fourier base functions present the advantage of being easy to compute and provide fast convergence in smooth cases.

We start our analysis by introducing the Fourier–Galerkin projection operator  $\pi_N$  onto the Fourier basis as follows:

$$\begin{aligned} \pi_N : X \times \mathbb{R} &\rightarrow X \times (\mathbb{Z}/(2N+1)\mathbb{Z}) \\ \pi_N(\mathbf{q}) &= \mathbf{q}_h(t) = \mathbf{q}_0 + \sum_{n=1}^N [\mathbf{q}_{c,n} \cos(n\omega t) + \mathbf{q}_{s,n} \sin(n\omega t)] \\ &= (\mathbf{Q}^{(\tau, N)})^T \mathcal{F}_N \end{aligned} \quad (2)$$

where  $\mathbf{Q}^{(\tau, N)}$  are the  $2N+1$  Fourier coefficients of the approximated solution  $\mathbf{q}_h$  and  $\mathcal{F}_N$  is the Fourier basis in sine/cosine components. The ansatz  $\mathbf{q}_h(t)$  and its derivative are smooth  $T$ -periodic functions.

#### 1. Fourier–Galerkin equations

So far, the procedure to obtain a periodic orbit remains general. Now, without loss of generality, we shall consider the case where the nonlinear flow is of quadratic type. This constraint is far from being restrictive since

---

\* javier.sierra@imft.com

many evolution problems can be recasted in this form, see Cochelin et al. [3] for the finite dimensional case. Fourier–Galerkin equations take the form form:

$$\begin{aligned} 0 &= \mathbf{L}\mathbf{q}_0 + \mathbf{N}_0 \\ n\omega\mathbf{B}\mathbf{q}_{n,s} &= \mathbf{L}\mathbf{q}_{n,c} + \mathbf{N}_{n,c}, \quad n = 1, \dots, N \\ -n\omega\mathbf{B}\mathbf{q}_{n,c} &= \mathbf{L}\mathbf{q}_{n,s} + \mathbf{N}_{n,s}, \quad n = 1, \dots, N \\ g_h(\mathbf{q}_h) &= 0. \end{aligned} \quad (3)$$

For the sake of brevity, Fourier coefficients  $\mathbf{N}_i$  are not developed as functions of  $\mathbf{Q}^{(\tau,N)}$ . Formally, eq. (3) will be denoted as:

$$\mathbf{0} = -\omega\tilde{\mathbf{B}}\mathbf{Q}^{(\tau,N)} + \tilde{\mathbf{L}}\mathbf{Q}^{(\tau,N)} + \tilde{\mathbf{N}}(\mathbf{Q}^{(\tau,N)}, \mathbf{Q}^{(\tau,N)}) = \tilde{\mathbf{r}}(\mathbf{Q}^{(\tau,N)}), \quad (4)$$

where operators  $\tilde{\mathbf{B}}$ ,  $\tilde{\mathbf{L}}$ , and  $\tilde{\mathbf{N}}(\cdot, \cdot)$  are block matrix operators. For more information the reader is referred to [4]

### B. Hill's method

The Fourier–Galerkin form of Floquet stability problem consists in the projection onto the finite Fourier space  $X \times (\mathbb{Z}/(2N+1)\mathbb{Z})$ , i.e. on a finite Fourier series.

The Floquet stability problem in the Fourier–Galerkin basis can be formally expressed with the following generalized eigenvalue problem:

$$\begin{aligned} \lambda^{(\tau,N)} \text{diag}(\mathbf{B})_{2N+1} \mathbf{P}^{(\tau,N)} &= D\tilde{\mathbf{r}}(\mathbf{Q}^{(\tau,N)}) \mathbf{P}^{(\tau,N)} \\ D\tilde{\mathbf{r}}(\mathbf{Q}^{(\tau,N)}) \mathbf{P}^{(\tau,N)} &= \left[ -\omega\tilde{\mathbf{B}} + \tilde{\mathbf{L}} + D\tilde{\mathbf{N}}(\mathbf{Q}^{(\tau,N)}) \right] \mathbf{P}^{(\tau,N)}, \end{aligned} \quad (5)$$

where  $\mathbf{P}^{(\tau,N)} = [\mathbf{p}_0, \mathbf{p}_{1,c}, \mathbf{p}_{1,s}, \dots, \mathbf{p}_{N,c}, \mathbf{p}_{N,s}]^T$  is the finite Fourier decomposition of the periodic eigenvector  $\mathbf{p}(t)$  and  $\lambda^{(\tau,N)}$  is the approximation of the Floquet exponent.

### C. Sensitivity analysis for periodic orbits

This section is an introduction to sensitivity computations near a bifurcation point of the periodic solution. Among possible applications to sensitivity theory, one may find passive control or identification of underlying physical mechanisms leading to the instability.

Let us consider the infinitesimal perturbed problem with respect to eq. (1):

$$\begin{aligned} \mathbf{B} \frac{\partial(\mathbf{q}^* + \delta\mathbf{q})}{\partial t} &= \mathbf{F}(\mathbf{q}^* + \delta\mathbf{q}, \nu) + \delta\mathbf{H}(\mathbf{q}^* + \delta\mathbf{q}), \\ \mathbf{q}^*(t + T) &= \mathbf{q}^*(t). \end{aligned} \quad (6)$$

A force-feedback perturbation  $\delta\mathbf{H}(\mathbf{q}^* + \delta\mathbf{q})$  leads to changes in dynamics. The original work of Giannetti et al. [5] analyzed the effect of a local force-feedback  $\delta\mathbf{H}(\delta\mathbf{q})$ . For that purpose, authors introduced the concept of *structural sensitivity* tensor  $\mathbf{S}_s$  to the secondary instability, i.e., a bifurcation of the Poincaré map associated to a  $T$ -periodic solution, which is the extension

of the structural sensitivity tensor of bifurcations from a steady-state solution, introduced by Giannetti et al. [6]. The structural sensitivity measures the variation of a Floquet exponent  $\delta\lambda$  with respect to variations in the Floquet mode  $\delta\mathbf{p}$ .

Let us begin with the averaged structural sensitivity tensor  $\bar{\mathbf{S}}_s$  of a Floquet exponent  $\lambda$ :

$$\bar{\mathbf{S}}_s(\mathbf{x}) = \frac{\int_t^{T+t} \mathbf{M}\mathbf{p} \otimes \mathbf{M}\mathbf{p}^\dagger dt}{\int_t^{T+t} \int_\Omega \mathbf{M}\mathbf{p} \cdot \mathbf{M}\mathbf{p}^\dagger d\mathbf{x} dt}. \quad (7)$$

It is the operator whose contraction with a generic infinitesimal localized feedback operator in space provides:  $\delta\lambda = \mathbf{C}_1 : \bar{\mathbf{S}}_s(\mathbf{x}_0)$ , where  $\delta\mathbf{H}(\delta\mathbf{q}) = \delta(\mathbf{x} - \mathbf{x}_0)\mathbf{C}_1 \cdot \delta\mathbf{q}$ , where  $\delta(\mathbf{x} - \mathbf{x}_0)$  is the Dirac distribution at  $\mathbf{x} - \mathbf{x}_0$  and  $\mathbf{C}_1$  is a generic constant feedback matrix. In the sensitivity paradigm, it is also helpful to consider phase details of the structural sensitivity which are retrieved by considering impulsive structural perturbations applied in time at a precise phase of the periodic solution, i.e., at  $t = t_0$ . This consideration leads to the instantaneous structural sensitivity  $\mathbf{S}_s$ :

$$\mathbf{S}_s(\mathbf{x}, t) = \frac{\mathbf{M}\mathbf{p} \otimes \mathbf{M}\mathbf{p}^\dagger}{\int_t^{T+t} \int_\Omega \mathbf{M}\mathbf{p} \cdot \mathbf{M}\mathbf{p}^\dagger d\mathbf{x} dt}. \quad (8)$$

In such a case, the variation of the Floquet exponent  $\delta\lambda = \mathbf{C}_1 : \mathbf{S}_s(\mathbf{x}_0, t_0)$ , where  $\delta\mathbf{H}(\delta\mathbf{q}) = \delta((t \bmod T) - t_0)\delta(\mathbf{x} - \mathbf{x}_0)\mathbf{C}_1 \cdot \delta\mathbf{q}$ , provides access to the phase. However, it fails to determine the harmonic nature of the instability. For such considerations, it is helpful to introduce a novel sensitivity map, the harmonic structural sensitivity  $\mathbf{S}_s^n$ , where  $n$  indicates the harmonic number. The direct computation of the frequency spectra  $\mathbf{S}_s^n$  is in general complex-valued. However, for the sake of self-consistency with the previous methodology,  $\mathbf{S}_s^{n,(s|c)}$  is the real harmonic structural sensitivity:

$$\begin{aligned} \mathbf{S}_s^{n,c}(\mathbf{x}) &= \frac{2}{T} \frac{\int_t^{T+t} \mathbf{M}\mathbf{p} \otimes \mathbf{M}\mathbf{p}^\dagger \cos(n\omega t) dt}{\int_t^{T+t} \int_\Omega \mathbf{M}\mathbf{p} \cdot \mathbf{M}\mathbf{p}^\dagger d\mathbf{x} dt} \\ \mathbf{S}_s^{n,s}(\mathbf{x}) &= \frac{2}{T} \frac{\int_t^{T+t} \mathbf{M}\mathbf{p} \otimes \mathbf{M}\mathbf{p}^\dagger \sin(n\omega t) dt}{\int_t^{T+t} \int_\Omega \mathbf{M}\mathbf{p} \cdot \mathbf{M}\mathbf{p}^\dagger d\mathbf{x} dt}, \end{aligned} \quad (9)$$

where the structural perturbation  $\delta\mathbf{H}(\delta\mathbf{q}) = \frac{2}{T} \cos(n\omega t)\delta(\mathbf{x} - \mathbf{x}_0)\mathbf{C}_1 \cdot \delta\mathbf{q}$ , resp.  $\sin(n\omega t)$ , provides a variation of the Floquet exponent  $\delta\lambda = \mathbf{C}_1 : \mathbf{S}_s^{n,c}(\mathbf{x}_0)$ , resp.  $\mathbf{S}_s^{n,s}(\mathbf{x}_0)$ , due to an harmonic perturbation. The  $\frac{2}{T}$  term is simply a normalization factor.

## II. RESULTS

### A. Flow past a two-dimensional circular cylinder

Let us consider a fluid mechanics example: a canonical case of the flow past a bluff body, i.e., the flow past a two-

dimensional cylinder sketched in fig. 1. Dynamics and the first two bifurcations are well known, see Williamson [7].

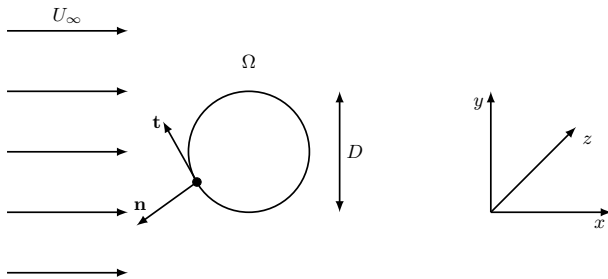


FIG. 1: Sketch of a cylinder immersed in a uniform flow.

### 1. Computation of the baseflow

The approach is initialized with the unstable eigenmode at threshold,  $Re \approx 47$ , and it is continued up to  $Re = 450$ , with at most  $N = 10$  modes. In order to estimate the precision of the results obtained by the numerical procedure, two Reynolds numbers are selected,  $Re = 190$  and  $Re = 260$ , and we run cross-comparison of the estimated Strouhal with the data available in literature. At  $Re = 190$  (resp.  $Re = 260$ ), by retaining  $N = 5$  harmonics, a Strouhal number  $St = 0.1938$  (resp.  $St = 0.2058$ ) has been obtained, a result in good agreement with the value  $St = 0.1950$  (resp.  $St = 0.2071$ ) reported by Barkley et al. [8]. These accurate results with a reduced Fourier basis are due to the rapid decay of the Fourier spectrum, which is displayed in fig. 2 (a). The Fourier spectrum displays a quadratic decay, with small dependence on the Reynolds number if sufficient modes are retained. To determine whether or not the number of retained modes is sufficient, one could evaluate a posteriori the evolution of the amplitude of each mode with respect to the parameter, i.e.,  $Re$ . Amplitude of each Fourier mode grows exponentially until saturation, see fig. 2 (b). Therefore, an appropriate selection of  $N$  could be to retain at least a mode that is not saturated or select the basis length  $N$  so that the amplitude of the last mode is below a certain threshold.

### 2. Performance evaluation of iterative methods

Another important aspect to be addressed is the performance of methods used for the numerical resolution. In particular, for the present case, authors have evaluated the dependency of the chosen iterative strategy, a flexible restarted GMRES, for the resolution of the underlying linear systems of the Newton iteration on a set of parameters: Reynolds number, preconditioning technique, and number of modes in the Fourier basis. Independently of the chosen preconditioning technique, the number of GMRES iterations for the resolution of the

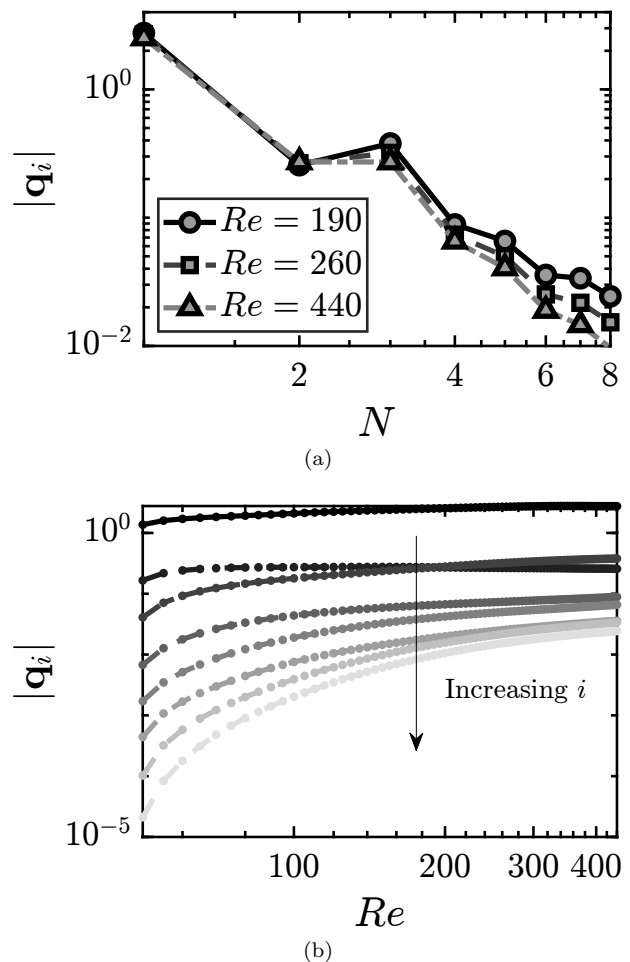


FIG. 2: (a) Decay of Fourier spectrum for  $Re = 190$ ,  $Re = 260$  and  $Re = 440$ , (b) evolution of the amplitude of Fourier modes.

linear system increases quadratically with respect to the Reynolds number, see fig. 3 (a). As expected, triangular Gauss-Seidel preconditioning speeds up computations with respect to block Jacobi. However, the gain between choosing an upper or a lower triangular preconditioner is marginal. In addition, authors have studied the effect of an inexact factorization of the inner diagonal blocks. ASM is used to precondition the inner blocks with upper triangular GS as outer preconditioner. It is compared with exact  $LU$  factorization for the diagonal blocks. It is concluded that inexact factorization of inner blocks hardly changes the number of GMRES iterations. The effect of the number of modes in the truncated Fourier basis is reported in fig. 3 (b). Similar conclusions can be drawn with respect to other preconditioners: the number of modes in the Fourier basis does not affect the iterative strategy, as long as  $N$  is sufficient for convergence.

In conclusion, GMRES iterations depend quadratically on the Reynolds number and they are independent on the dimension of the Fourier basis as long as  $N$  is sufficient to characterize the periodic solution. In a future study,

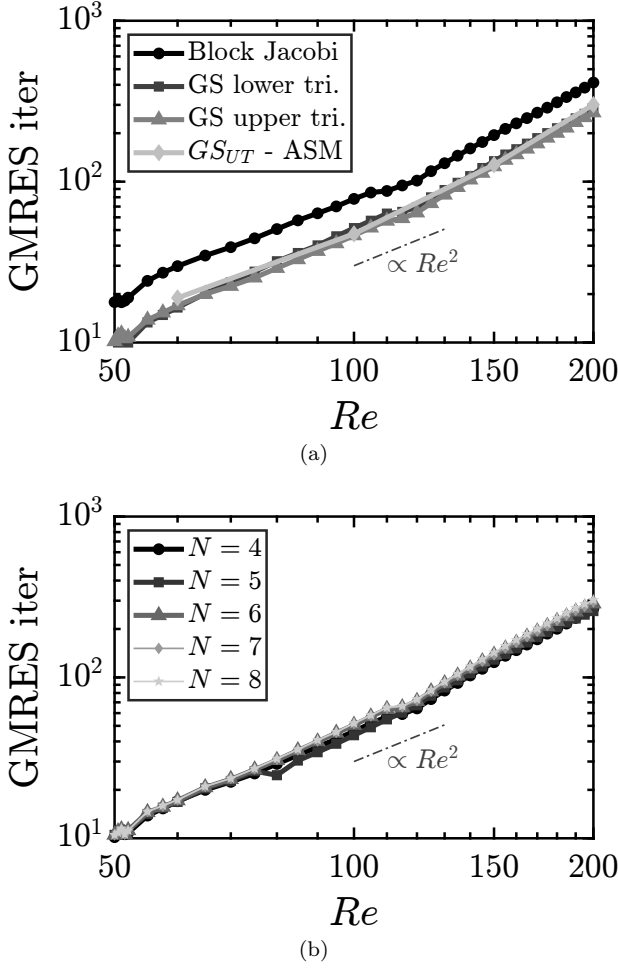


FIG. 3: Effect of Reynolds number, preconditioning technique and number of Fourier modes. (a) compares preconditioning techniques and (b) the number of Fourier modes for a Gauss–Seidel upper triangular preconditioner.

authors will study other preconditioning techniques to attempt to reduce the dependency on  $Re$ .

### 3. Stability & sensitivity analysis

Beyond the threshold of the first instability, which is found at around  $Re \approx 47$ , a stable two-dimensional  $T$ -periodic solution exists up to  $Re \approx 190$  where the stable solution ceases to be two-dimensional via a steady symmetry-breaking bifurcation of the spanwise homogeneous direction. The Floquet mode associated to this second instability, reported in fig. 4, is commonly denoted as *mode A* whose wavenumber is  $k_z = 1.585$  [5].

Prior to the discussion of sensitivity quantities, let us point out their validity. The reported sensitivity maps in fig. 5 are in perfect agreement with those presented in literature, cf. [9]. A common query in physics is: which are the underlying physical mechanisms responsible for

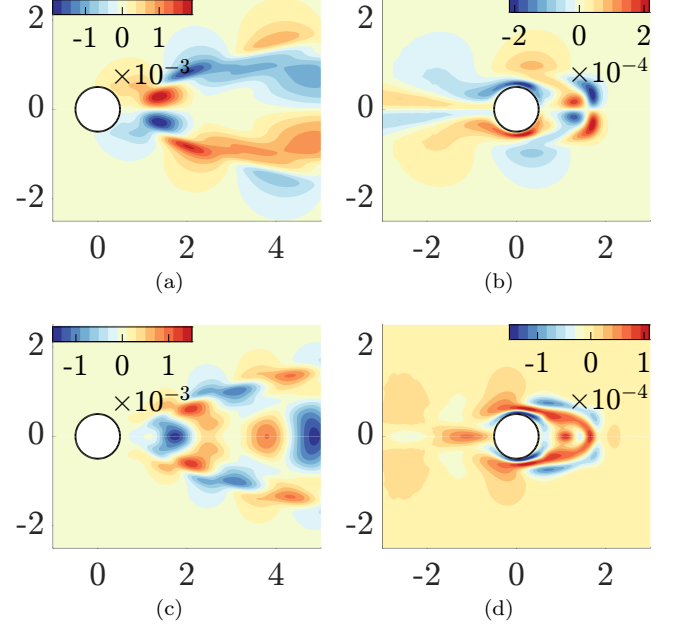


FIG. 4: Spanwise velocity component  $U_z$  of *mode A* at  $Re = 190$ . (a) and (c), resp. (b) and (d), first and second sinus components of direct, resp. adjoint, Floquet modes.

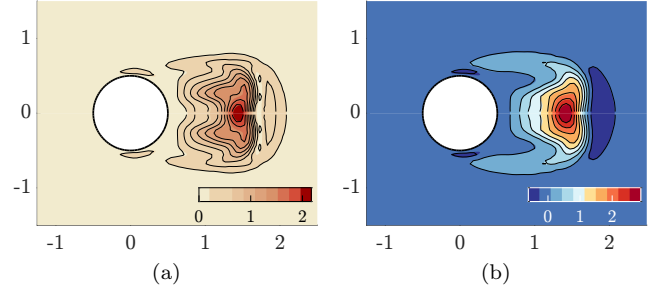


FIG. 5: Averaged structural sensitivity  $\bar{S}_s^{(\tau, N)}$  of mode A at  $Re = 190$ ,  $k_z = 1.585$ , and  $N = 4$ . (a) Spectral norm, (b) trace.

the instability? Structural sensitivity allows to localize the core of the vortex-shedding instability, that is the sensitivity of the Floquet exponent to a generic structural perturbation of the linearized equations. Figure 5 displays the compact support structure of the sensitivity for mode A, which translates to a localized instability in the near wake.

### ACKNOWLEDGMENTS

I wish to acknowledge the support of the P. Jolivet with the PETSc/SLEPc interface and to V. Citro and F. Giannetti for their support in this study.

- 
- [1] M. Urabe, Galerkin's procedure for nonlinear periodic systems, *Arch. Rational Mech. Anal.* **20**, 120 (1965).
  - [2] M. Krack and J. Gross, *Harmonic balance for nonlinear vibration problems* (Springer, 2019).
  - [3] B. Cochelin and C. Vergez, A high order purely frequency-based harmonic balance formulation for continuation of periodic solutions, *Journal of sound and vibration* **324**, 243 (2009).
  - [4] J. Sierra, P. Jolivet, V. Citro, and F. Giannetti, Adjoint-based sensitivity analysis of periodic orbits by the fourier–galerkin method, Manuscript submitted for publication (2020).
  - [5] F. Giannetti, S. Camarri, and P. Luchini, Structural sensitivity of the secondary instability in the wake of a circular cylinder, *Journal of Fluid Mechanics* **651**, 319 (2010).
  - [6] F. Giannetti and P. Luchini, Structural sensitivity of the first instability of the cylinder wake, *Journal of Fluid Mechanics* **581**, 167 (2007).
  - [7] C. H. K. Williamson, Vortex dynamics in the cylinder wake, *Annual review of fluid mechanics* **28**, 477 (1996).
  - [8] D. Barkley and R. D. Henderson, Three-dimensional floquet stability analysis of the wake of a circular cylinder, *Journal of Fluid Mechanics* **322**, 215 (1996).
  - [9] F. Giannetti, S. Camarri, and V. Citro, Sensitivity analysis and passive control of the secondary instability in the wake of a cylinder, *Journal of Fluid Mechanics* **864**, 45 (2019).